

# Online Evasive Strategy for Aerial Survey using Sierpinski curve

Ashay Wakode \* Arpita Sinha \*\*

\* Indian Institute Of Technology Bombay, Mumbai, Maharashtra 400076 India (e-mail: ashaywakode@gmail.com).

\*\* Indian Institute Of Technology Bombay, Mumbai, Maharashtra 400076 India (e-mail: arpita.sinha@iitb.ac.in)

**Abstract:** This paper deals with the aerial survey of a closed region using the Space-Filling curve, particularly Sierpinski curve. The specified region is triangulated, and the Sierpinski curve is used to explore each smaller triangular region. The entire region may have one or more obstacles. An algorithm is presented which suggests evasive manoeuvre (detour) if an obstacle is detected. The algorithm is online; that is, it does not require prior knowledge of the location of obstacles and can be applied while the robotic system is traversing the designated path. The fractal nature of the Sierpinski curve and simple geometric observations were used to formulate and validate the algorithm. The non-uniform coverage and multiple obstacle problems are also dealt with towards the end.

**Keywords:** Autonomous Vehicles, Coverage Path Planning, Online Obstacle evasion, Robotic Exploration, Space-Filling curve, Trajectory and Path Planning

## 1. INTRODUCTION

Space-Filling curves are a special type of curves that pass through every point of closed interval onto which they are mapped. Space-Filling curves are made out of smaller similar curves, which is referred to as the fractal nature of space filling curves (Sagan (1994), Bader (2012)). Due to these interesting properties, space-filling curves are widely used in applications where the agent needs to explore/survey a region and gather data. Other applications of Space-Filling curves can be found in computer graphics (Dafner et al. (2000), Memon et al. (2000)), Computer Aided-Design (Bader (2012)), parallel computing (Zumbusch (2000)) and many more.

With advent of Unmanned Aerial Vehicles (UAVs), the robotics exploration/survey task has been simplified. Survey using UAVs is superior due to the following advantages :

- (1) The search agent no longer need to worry about the region's topography.
- (2) The surface of the region being explored remains undisturbed.
- (3) Cheaper and less bulky UAVs can be deployed in huge numbers, reducing cost and increasing efficiency in terms of both energy and time.

A survey of a region using aerial vehicles is theoretically better but requires robust algorithms/strategies for implementation in the real world. This paper deals with one such strategy for aerial survey using the Sierpinski curve.

The robotics exploration problem is a sub-problem of the Coverage Path Planning problem (CPPP). In CPPP, a robotic agent needs to traverse through a certain region while doing tasks like mowing, painting, or cleaning, to

name a few. There are many solutions available for CPPP which can be used for robotic exploration problem and hence for aerial survey: Boustrophedon decomposition, Grid-based methods, Graph-based methods, and many more (Galceran and Carreras (2013)).

Space-Filling curves provide a novel solution to robotic exploration problem because of their useful properties. An exhaustive search can be carried out since it passes through every point of the region. The fractal nature allows us to design algorithms/strategies easily since a space-filling curve is a combination of other similar space-filling curves. Space-Filling curves can span both 2D and 3D space, and algorithms built for a 2D region can be easily extended to 3D space.

Spires and Goldsmith (1998) suggest the use of a swarm of robots for exploration, each robot following a space-filling curve. This approach is efficient in terms of energy, robust to failures, and assures coverage in finite time, But the presence of obstacles is not considered. Tiwari et al. (2007) and Ban et al. (2013) propose a solution to the exploration problem using a space-filling curve. However, apriori location of obstacles is required making them unsuitable for online implementation. Nair et al. (2017), Joshi et al. (2019) give out online algorithms for robotic exploration using Hilbert's space-filling curve. However, the obstacles must occupy only single and double neighboring grid locations. But, this approach cannot be used for the Sierpinski curve. So, No online exploration strategy exists for an agent following a Sierpinski curve.

We have formulated a strategy for aerial survey when the search agent uses the Sierpinski curve as a guiding path while avoiding obstacles; when the location of obstacles is unknown. The suggested strategy is online; that is,

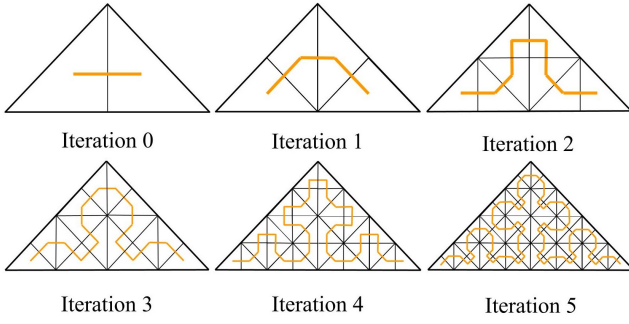


Fig. 1. First 6 iterations of the Sierpinski curve shown using yellow piece-wise straight line

the whereabouts of the obstacles are unknown when the search is initiated, and the strategy comes into play once it detects the obstacles. The details of strategy implementation in multiple obstacle situations and non-uniform coverage scenarios are established. Finally, the strategy is put together as a pseudo-code for real-life applications.

Section 2 introduces various preliminaries on the Sierpinski curve and other tools required in the following sections. Section 3 formulates the problem and presents the strategy. Various lemmas for validating the result are produced in this section. Section 4 touches upon multiple obstacle scenarios. Section 5 gives out the pseudo-code for implementation of the strategy, and the non-uniform coverage problem is dealt with in brief. Lastly, Section 6 concludes the paper.

## 2. PRELIMINARIES

### 2.1 Sierpinski Curve

Sierpinski curve is a mapping from  $\mathbf{I} = [0, 1]$  to  $\mathbf{T}$ , where  $\mathbf{T} = \{(\mathbf{x}, \mathbf{y}) : \mathbf{y} \geq \mathbf{0}, \mathbf{x} - \mathbf{y} \geq \mathbf{0}, \mathbf{x} + \mathbf{y} - 2 \leq \mathbf{0}\}$  (1)

In this paper, we will use approximations of the Sierpinski curve. The approximate Sierpinski curve can be constructed by dividing  $\mathbf{T}$  into smaller triangles and connecting them in a certain fashion, see figure 1.  $\mathbf{I}$  is also divided into smaller sub-intervals, which are then mapped to the smaller sub-regions, see figure 2. Here, the refinement of tessellation used for constructing the Sierpinski curve is quantified by iteration number (denoted as  $n$ ). In figure 1,  $n = 1$  Sierpinski curve has right triangle divided  $2^2 = 4$  times,  $n = 2$  Sierpinski curve has right triangle divided  $2^3 = 8$  times, and so on. As  $n \rightarrow \infty$ , approximate Sierpinski curve tends to Sierpinski curve.

A robotic agent with point size sensing radius will require to follow the Sierpinski curve with iteration number going to  $\infty$ . However, a search agent with a finite non-zero sensing radius going from one center of triangle to another following the approximate Sierpinski curve can explore  $\mathbf{T}$  entirely, given it can explore the entire triangular cell it is present in.

### 2.2 Grammar-based construction of Sierpinski curve

The fractal nature of the Sierpinski curve can be used for its construction. Consider patterns  $S$ ,  $Z$ ,  $R$ , and  $P$ ,

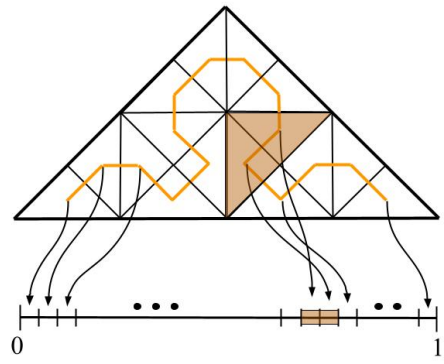


Fig. 2. Mapping between  $\mathbf{I}$  and  $\mathbf{T}$

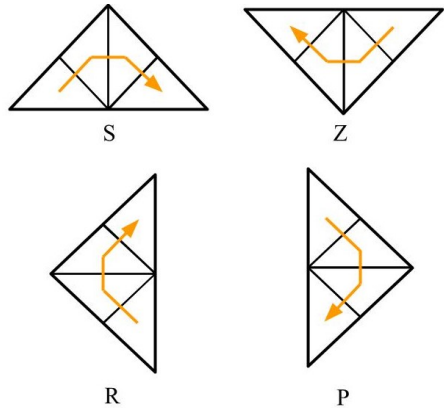


Fig. 3. Patterns  $S$ ,  $Z$ ,  $R$ , and  $P$

as shown in figure 3. Here,  $S$  is the  $n = 1$  iteration of Sierpinski curve. Now, using the following production rules, further odd-numbered iterations of the Sierpinski curve can be constructed:

$$S \Rightarrow S \nearrow R \rightarrow P \searrow S \quad (2)$$

$$R \Rightarrow R \nwarrow Z \uparrow S \nearrow R \quad (3)$$

$$Z \Rightarrow Z \swarrow P \leftarrow R \nwarrow Z \quad (4)$$

$$P \Rightarrow P \searrow S \downarrow Z \swarrow P \quad (5)$$

Higher iterations can be constructed in the following way:

$$\begin{aligned} n = 1 : & S \\ n = 3 : & S \nearrow R \rightarrow P \searrow S \\ n = 5 : & (S \nearrow R \rightarrow P \searrow S) \nearrow (R \nwarrow Z \uparrow S \nearrow R) \rightarrow \\ & (P \searrow S \downarrow Z \swarrow P) \searrow (S \nearrow R \rightarrow P \searrow S) \end{aligned}$$

Similar patterns and production rules exist for even-numbered iteration Sierpinski curves (Bader (2012)).

There is another way to look at the fractal nature of the Sierpinski curve. It is easy to observe that the iteration 2 Sierpinski curve can be obtained by putting two iteration 1 Sierpinski curves along the shorter side symmetrically and joining the ends. To generalize, iteration  $n$  Sierpinski curve can be obtained by combining two iteration  $n-1$  Sierpinski curves. It is not hard to prove the previous statement. The patterns and the production rules introduced previously can be easily used to prove the statement.

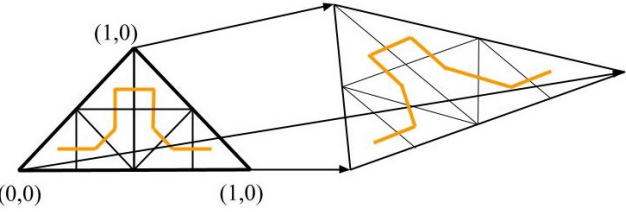


Fig. 4. Projective Transformation

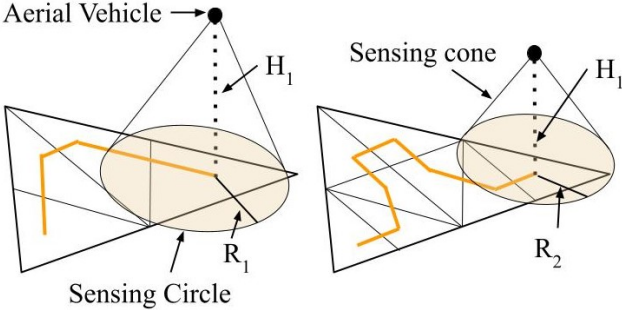


Fig. 5. Sensing mechanism of the aerial vehicle is of the form of a cone, sensing radius on ground can be changed by varying height,  $H_1 > H_2 \implies R_1 > R_2$

### 2.3 Extension to Generalised Sierpinski curve

The Sierpinski curve generated in the previous subsection spans an isosceles right triangle ( $\mathbf{T}$ ). However, we are interested in the Sierpinski curve spanning a random triangle, referred to as the Generalised Sierpinski curve (abbreviated as GSc). Patterns and production rules similar to the ones introduced in the last subsection exists for GSc.

Working with GSc using patterns and production rules can get complicated. Instead we introduce a simple method for generating GSc. Here, the Sierpinski curve for  $\mathbf{T}$  is generated and converted to GSc spanning a known triangle (denoted as  $\mathbf{U}$ ) using projective transformation (see Kanatani et al. (2016)), as shown in figure 4. Projective transformation is a linear map given by equation 6.

$$\begin{bmatrix} x' \\ y' \\ 1 \end{bmatrix} = \begin{bmatrix} \alpha & \beta & \gamma \\ \epsilon & \zeta & \eta \\ 0 & 0 & 1 \end{bmatrix} \begin{bmatrix} x \\ y \\ 1 \end{bmatrix} \quad (6)$$

Here,  $(x, y) \in \mathbf{T}$  mapped to  $(x', y') \in \mathbf{U}$ .  $\alpha, \beta, \gamma, \epsilon, \zeta$  and  $\eta$  are constants for given  $\mathbf{U}$ , and can be calculated by mapping vertices of  $\mathbf{U}$ , which are already known.

## 3. MAIN RESULT

### 3.1 Problem Formulation

The search agent, which in this case is an aerial vehicle, travels through  $\mathbf{U}$  using the path marked by GSc. The sensing radius of the search agent and the iteration of GSc are to be decided by the user. The sensing radius and the iteration of GSc are chosen such that the search agent is able to search the entire triangular cell it is present in (See figure 5). The iteration of GSc depends on how rigorously the user wants the search agent to survey a certain part of the region (Further details can be found in Section 5).

In this paper, we assume the obstacles to block single triangular cells in the GSc, and that the search agent

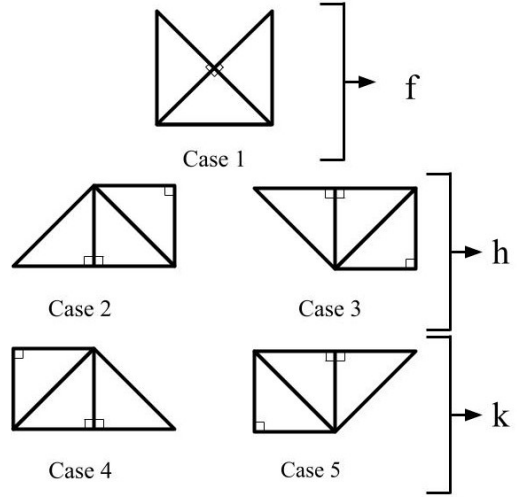


Fig. 6. Possible geometries of 3 consecutive triangular cells in  $\mathbf{T}$

detects those obstacles before bumping into them. We further assume that the search agent is equipped with a sensing mechanism to detect obstacles.

While traversing the GSc, the search agent at  $i^{th}$  triangular cell detects obstacle at  $i + 1^{th}$  triangular cell. So, the search agent has to go around the obstacle cell to reach  $i + 2^{th}$  triangular cell and thus successfully evade the obstacle. The search agent may have multiple choices of evasive maneuvers, and the best will be the least lengthy.

So, the problem boils down to planning evasive maneuvers between the  $i^{th}$  and  $i + 2^{th}$  triangular cells, with the  $i + 1^{th}$  cell blocked by an obstacle. The possible cases of 3 consecutive triangular cell geometries in the Sierpinski curve are listed in figure 6.

*Lemma 1.* Case 1-5 are the only possible 3 consecutive triangular cell geometries in the Sierpinski curve.

**Proof.** The fractal nature of Sierpinski curve can be used here. It is easy to observe that the case 2-5 are the only cases possible in pattern  $S$ ,  $R$ ,  $Z$  and  $P$ . Finally, the geometries generated after joining  $S$ ,  $R$ ,  $Z$  and  $P$  also contains case 1-5 only. Therefore, cases 1-5 are the only possible 3 consecutive triangular geometries in the Sierpinski curve. ■

Since projective transformation is a linear map, the previous statement also holds for GSc, with the perpendicular bisectors in cases 1-5 turning into medians (Line joining a vertex to the mid-point of the opposite side).

Here, case 1 is tagged  $f$ . Cases 2 and 3 are similar; since they are water images, they are tagged as  $h$ . Similarly, Cases 4 and 5 are tagged as  $k$ . Finally, some nomenclature:

- (1)  $W_i$  : Centre of the  $i^{th}$  triangular cell.
- (2)  $C$  : Common vertex shared by all 3 triangular cells in each case 1-5.
- (3)  $B_{i,j}$  : Vertex shared by  $i^{th}$  and  $j^{th}$  triangular cells only.
- (4)  $D_{i,j}$  : Vertex of  $i^{th}$  triangular cell not shared with  $j^{th}$  triangular cell.

**Algorithm 1.** Algorithm for tag generation

```

1: Input :  $i, C, D_{i,i+1}, D_{i+1,i}, B_{i,i+1}$ 
2: Output : Tag
3: if  $A(D_{i,i+1}, C, D_{i+1,i}) = 0$  then
4:   Tag is  $f$ 
5: else if  $A(D_{i,i+1}, B_{i,i+1}, D_{i+1,i}) = 0$  then
6:   Tag is  $h$ 
7: else
8:   Tag is  $k$ 
9: end if

```

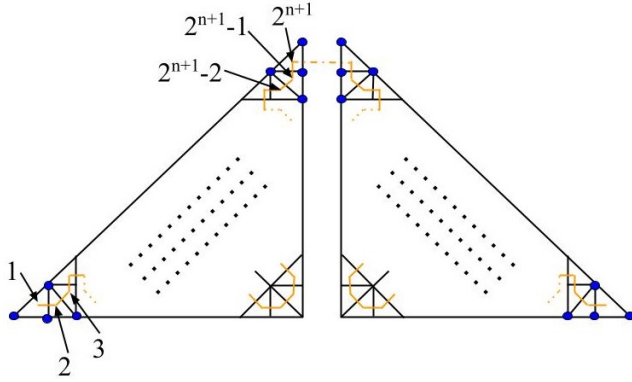


Fig. 7. Combination of two  $n = 2k + 1$  iteration Sierpinski curve to get  $n = 2k + 2$  iteration Sierpinski curve; Vertices of interest are highlighted in blue; Triangular cells of interest are numbered; Easy to see lemma 2 holds for both

Finally, algorithm 1 can be used to tag 3 consecutive triangular cells beginning with  $i^{th}$  cell.

### 3.2 Proposed Strategy and Validity of Proposed Strategy

Evasive maneuvers are proposed in Table 1.  $L$  quantifies the length of maneuvers. Case 2 has been used for visualizing maneuvers for tag  $h$ . Case 4 has been used for visualizing maneuvers for tag  $k$ . The algorithm for online implementation is presented in Section 5.

**Lemma 2.** Only the first two and the last two triangular cells in GSc have all three vertices on the boundary of  $\mathbf{U}$ . Also, only  $2^{nd}$  and  $3^{rd}$  triangular cells (both from start and end of GSc) share two vertices, both of which lie on the boundary.

**Proof.** The lemma is proved for the Sierpinski curve spanning  $\mathbf{T}$ . Since the transformation from  $\mathbf{T}$  to  $\mathbf{U}$  is linear, the statement would hold for GSc.

Using mathematical induction. Lemma holds for  $n = 1, 2$ . Using fractal nature of the Sierpinski curve, iteration  $n = 2k+2$  (even) Sierpinski curve can be constructed using two  $n = 2k+1$  iteration Sierpinski curves, and interestingly lemma holds in both cases (See figure 7). Similar argument holds for  $n = 2k + 1$  (odd) as well. Therefore, the lemma holds. ■

**Lemma 3.** Using the evasive strategies enlisted in Table 1, a search agent can evade any obstacle lying entirely inside a single triangular cell, except when the obstacle is present inside the one of first 3 or last 3 triangular cells of GSc.

**Proof.** Table 1 lists evasive techniques for nodes with tags  $f, h$  and  $k$ . The tags are given to geometries of cases 1 to 5

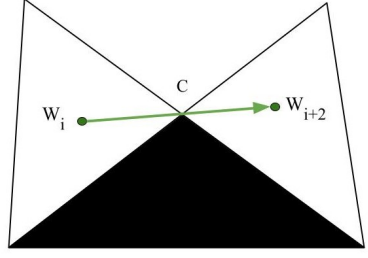


Fig. 8. Tag  $f$  geometry

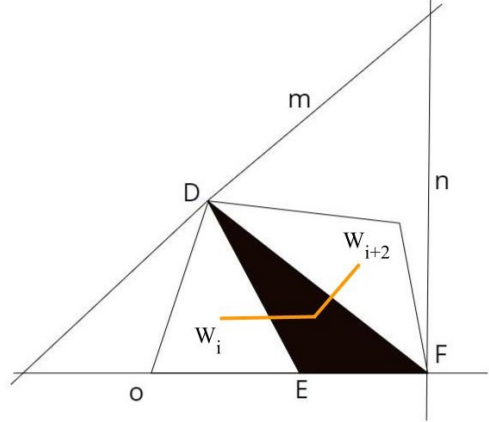


Fig. 9. Tag  $h$  geometry; Obstacle represented by black triangular cell

(refer figure 6). Cases 1-5 are the only possible geometries of three consecutive triangular cells in GSc, as proved in lemma 1. So, it remains to be shown that strategies enlisted in table 1 are always possible for each tag. Hence, the following cases :

- (1) Tag  $f$  (See figure 8) : This will be impossible if  $C$  lies on the boundary. Assuming  $C$  lies on the boundary, there would be two line segments originating from  $C$  with an interior angle  $> 180^\circ$ , which is infeasible. Hence  $C$  will never lie on the boundary. Therefore, the evasive strategy for this case will always be possible.
- (2) Tag  $h$  (See figure 9) : Let the cell with the obstacle be denoted as  $\Delta DEF$ . The possible boundary lines which can stop the search agent from following the evasive maneuvers are labeled as  $m, n$ , and  $o$ .

Firstly, assume only lines  $o$  and  $m$  are present. Then the cell preceding  $\Delta DEF$  will have all of its vertices on the boundary, and hence it will be either  $1^{st}$  or  $2^{nd}$  cell from start or end (from lemma 2), which implies  $\Delta DEF$  will be  $2^{nd}$  or  $3^{rd}$  cell; this contradicts the assumption that the cell with an obstacle is not one of the first or last three cells in GSc.

Secondly, assume only lines  $o$  and  $n$  are present. In this situation, the robotic system can follow the evasive strategy 2.

Thirdly, assume only lines  $m$  and  $n$  are present. Here,  $\Delta DEF$  and the succeeding triangle share two vertices that lie on the boundary. This implies  $\Delta DEF$  is either the  $2^{nd}$  or  $3^{rd}$  cell from start or end (from lemma 2). Therefore, a contradiction.

Table 1. Evasive Strategies

Sr. No.	Evasive Maneuver	Change of Path	$L$
1		$w_i \rightarrow C \rightarrow w_{i+2}$	$L_1 = \frac{ C-w_i + w_{i+2}-C }{ w_{i+2}-w_i }$
2		$w_i \rightarrow C \rightarrow w_{i+2}$	$L_2 = \frac{ C-w_i + w_{i+2}-C }{ w_{i+2}-w_i }$
3		$w_i \rightarrow B_{i,i+1} \rightarrow B_{i+1,i+2} \rightarrow w_{i+2}$	$L_3 = \frac{ B_{i,i+1}-w_i + B_{i+2,i+1}-B_{i,i+1} + w_{i+2}-B_{i+2,i+1} }{ w_{i+2}-w_i }$
4		$w_i \rightarrow C \rightarrow w_{i+2}$	$L_4 = \frac{ C-w_i + w_{i+2}-C }{ w_{i+2}-w_i }$
5		$w_i \rightarrow B_{i,i+1} \rightarrow B_{i+1,i+2} \rightarrow w_{i+2}$	$L_5 = \frac{ B_{i,i+1}-w_i + B_{i+2,i+1}-B_{i,i+1} + w_{i+2}-B_{n+2,n+1} }{ w_{i+2}-w_i }$

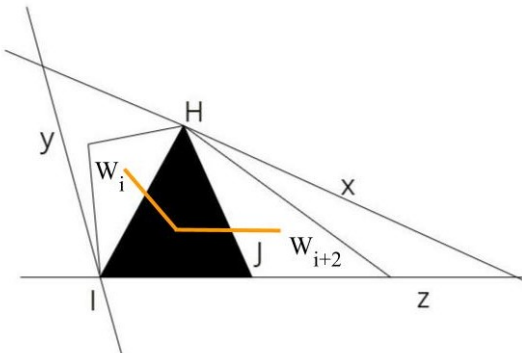


Fig. 10. Tag  $k$  geometry; Obstacle represented by black triangular cell

Lastly, assuming the presence of all lines  $o$ ,  $m$ , and  $n$  will imply that  $\Delta DEF$  is the  $2^{nd}$  triangle from start or end (from lemma 2). Again, a contradiction.

(3) Tag  $k$  (See figure 10) : Proceeding on the same lines, Let the cell with the obstacle be denoted as  $\Delta H I J$ . The possible boundary lines which can stop the search agent from doing an evasive maneuver are labeled as  $x$ ,  $y$ , and  $z$ .

Firstly, assume only lines  $x$  and  $z$  are present. The cell succeeding  $\Delta H I J$  will have all of its vertices on

the boundary, and hence it will be either  $1^{st}$  or  $2^{nd}$  cell from start or end (from lemma 2), hence  $\Delta H I J$  will be  $2^{nd}$  or  $3^{rd}$  cell. A contradiction.

Secondly, assume only lines  $x$  and  $y$  are present. In this situation, the robotic system can follow evasive strategy no. 4.

Thirdly, assume only lines  $y$  and  $z$  are present. Here,  $\Delta H I J$  and the preceding cell share two vertices which lie on the boundary. Which implies  $\Delta H I J$  is either  $2^{nd}$  or  $3^{rd}$  triangle from start or end (from lemma 2). Therefore, a contradiction. Lastly, assuming the presence of all lines  $x$ ,  $y$ , and  $z$  will imply that  $\Delta D E F$  is  $2^{nd}$  cell from start or end (from lemma 2). Again, a contradiction.

Therefore, The lemma is proved.  $\blacksquare$

#### 4. MULTIPLE OBSTACLE SCENARIO

The strategy presented can be extended to situations wherein multiple obstacles are present. The alternate path for evading a single obstacle depends only on the triangular cells preceding and after the triangle with an obstacle. So, if the  $j^{th}$  triangular cell has an obstacle, then the strategy presented will not work if the  $j + 1^{th}$  triangle also has an obstacle. Nevertheless, the strategy can be applied in a usual way if the  $j + 2^{th}$  triangle has an obstacle. So, the

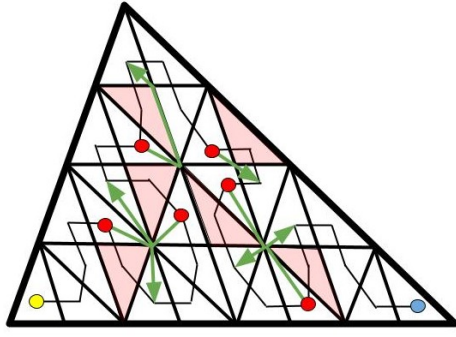


Fig. 11. Triangle explored using iteration 4 Sierpinski curve; Red triangular cells: locations blocked by obstacles; Red points: locations at which obstacle is detected and the evasive maneuver is initiated.

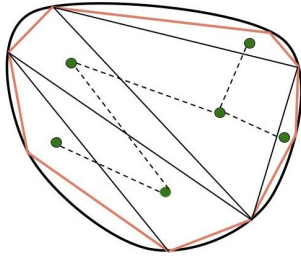


Fig. 12. Black closed curve: Region to be explored; Brown Polygon: Approximate Polygon with triangulation; Dark green vertices and dashed edges: Graph to be explored

strategy will work for any number of disjoint obstacles. This is shown in figure 11.

## 5. IMPLEMENTATION & NON-UNIFORM COVERAGE SCENARIO

### 5.1 Real-life Implementation

Sierpinski curve explores a triangle, but in real life, the region to be explored may not be a triangle. It will be a closed curve. A closed region can be approximated by polygon (referred to as  $P$ ) using fast and efficient algorithms; see Sklansky and Gonzalez (1980).  $P$  can be triangulated to get  $T_P$ , using existing methods with time complexity of  $O(n \log n)$  for Siedel's method (Seidel (1991)),  $O(n)$  for Toussaint's method (Toussaint (1984)), and many more. The choice of method for triangulation rests with the user.

A dual graph  $G(T_P)$  of  $T_P$  is generated. A dual graph of a triangulated polygon is a graph with vertices for triangles, and the vertices denoting triangles sharing sides are joined using edges (Berg et al. (1997)). Lastly, exploring the entire region will need the search agent to visit vertices of  $G(T_P)$  and use the Sierpinski curve to explore the triangles denoted by vertices. Traversing between the vertices of  $G(T_P)$  will be a Traveling Salesman Problem, whose solution can be found offline (see Figure 12).

The aerial survey of a scalene triangle using the Sierpinski curve requires function  $Y$ , which goes to zero on the edges, and is non-zero everywhere.  $Y$  can be formulated

### Algorithm 2. Algorithm for online implementation

```

1: Input :  $n$ , Search agent at  $i^{th}$  cell, Obstacle detected
   at  $i + 1^{th}$  cell,  $C$ ,  $B_{i,i+1}$ ,  $B_{i+1,i+2}$ 
2: Output : Detour to get to  $i + 2^{th}$  triangular cell
3: if  $Tag(i) = f$  then
4:   Follow strategy 1 from Table 1
5: end if
6: if  $Tag(i) = h$  then
7:   if  $Y(C) \neq 0$  then
8:     if  $L_2 < L_3$  then
9:       Follow strategy 2 from Table 1
10:    else if  $Y(B_{i,i+1}) \times Y(B_{i+1,i+2}) \neq 0$  then
11:      Follow strategy 3 from Table 1
12:    end if
13:   else
14:     Follow strategy 3 from Table 1
15:   end if
16: end if
17: if  $Tag(i) = k$  then
18:   if  $Y(C) \neq 0$  then
19:     if  $L_4 < L_5$  then
20:       Follow strategy 4 from Table 1
21:     else if  $Y(B_{i,i+1}) \times Y(B_{i+1,i+2}) \neq 0$  then
22:       Follow strategy 5 from Table 1
23:     end if
24:   else
25:     Follow strategy 5 from Table 1
26:   end if
27: end if

```

by multiplying line equations of edges of the triangle. Function  $Y$  ensures that the robotic system does not cross the boundary and go out of the region to be explored. Assuming the search agent at the  $i^{th}$  triangular cell, and obstacle is detected at  $i + 1^{th}$  triangular cell. Using  $Y$ , algorithm 2 gives a path to be followed to  $i + 2^{th}$  triangular cell.

### 5.2 Non-Uniform Coverage

In robotic exploration scenarios, the search agent may have some prior knowledge about the region. Search agent may be aware of certain parts of the region that have a higher probability of discovering entities of interest like minerals or resources. In such a situation, it is wise for the search agent to explore the higher probability parts rigorously, giving those parts more time and surveying them more closely. Such scenarios are referred to as Non-Uniform Coverage Planning.

Sadat et al. (2014) discusses non-uniform coverage scenarios in aerial survey. Sadat et al. (2015) go a step forward and use Hilbert's space filling curve for exploration. Finally, with Hilbert's space-filling curve, Nair et al. (2017) introduced strategies for obstacle evasion in a non-uniform coverage context.

This paper investigates obstacle evasion for the Sierpinski curve in non-uniform scenarios using strategy presented in Section 3. The parts of the region which are required to be explored rigorously are traversed using a higher iteration Sierpinski curve, Which allows the aerial vehicle to spend more time on such parts. Nevertheless, the distance between surface of the region and the aerial

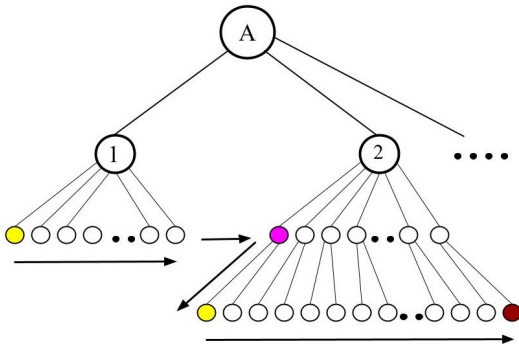


Fig. 13. Shortcut Heuristic

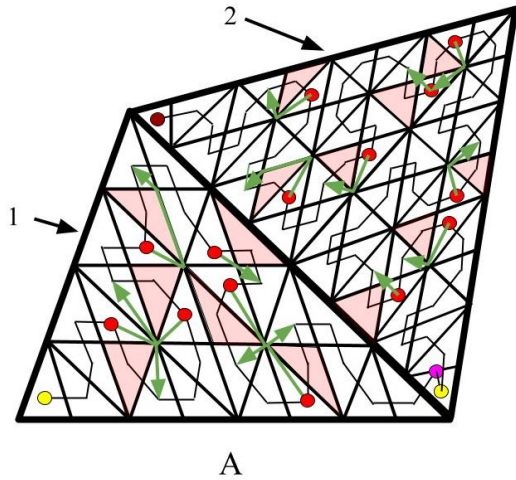


Fig. 14. Non-Uniform Coverage of region A, with 1 and 2 as parts; Search agent jumps to the purple point while going from 1 to 2, then goes to yellow point to start exploring 2, due to SH

vehicle reduces as sensing radius is reduced, implying lesser loss of information due to errors.

Here, we use Shortcut Heuristic (denoted as SH) for traveling between parts (see Sadat et al. (2014)). In SH, a search agent visits all the triangular cells at the lowest level of a part, then visits the nearest triangular cell of the next part and goes on visiting all the triangular cells at the lowest level in that part; this is done recursively to cover the entire region (See figure 13). Finally, figure 14 shows an example of non-uniform coverage using the Sierpinski curve.

## 6. CONCLUSION

The Aerial Survey problem using the Sierpinski curve has been considered. Strategies to evade obstacles online were presented. Simple geometric properties were used to devise evasive strategies. The suggested strategies introduced are proven to be exhaustive. The evasion plan is also shown to be helpful in non-uniform coverage situations. The strategy can be used for two or more disjoint obstacles covering triangular cells of the Sierpinski curve. The presented strategy cannot be used for obstacles covering two or more arbitrary triangular cells, but this can be a good starting point. Hence further work demands consideration of arbitrary sized and shaped obstacles.

## REFERENCES

Bader, M. (2012). *Space-filling curves: an introduction with applications in scientific computing*, volume 9. Springer Science & Business Media.

Ban, X., Goswami, M., Zeng, W., Gu, X., and Gao, J. (2013). Topology dependent space filling curves for sensor networks and applications. In *2013 Proceedings IEEE INFOCOM*, 2166–2174. IEEE.

Berg, M.d., Kreveld, M.v., Overmars, M., and Schwarzkopf, O. (1997). Computational geometry. In *Computational geometry*, 1–17. Springer.

Dafner, R., Cohen-Or, D., and Matias, Y. (2000). Context-based space filling curves. In *Computer Graphics Forum*, volume 19, 209–218. Wiley Online Library.

Galceran, E. and Carreras, M. (2013). A survey on coverage path planning for robotics. *Robotics and Autonomous systems*, 61(12), 1258–1276.

Joshi, A.A., Bhatt, M.C., and Sinha, A. (2019). Modification of hilbert's space-filling curve to avoid obstacles: A robotic path-planning strategy. In *2019 Sixth Indian Control Conference (ICC)*, 338–343. IEEE.

Kanatani, K., Sugaya, Y., and Kanazawa, Y. (2016). *Guide to 3D Vision Computation*, volume 3. Springer.

Memon, N., Neuhoff, D.L., and Shende, S. (2000). An analysis of some common scanning techniques for lossless image coding. *IEEE transactions on image processing*, 9(11), 1837–1848.

Nair, S.H., Sinha, A., and Vachhani, L. (2017). Hilbert's space-filling curve for regions with holes. In *2017 IEEE 56th annual Conference on decision and control (CDC)*, 313–319. IEEE.

Sadat, S.A., Wawerla, J., and Vaughan, R. (2015). Fractal trajectories for online non-uniform aerial coverage. In *2015 IEEE international conference on robotics and automation (ICRA)*, 2971–2976. IEEE.

Sadat, S.A., Wawerla, J., and Vaughan, R.T. (2014). Recursive non-uniform coverage of unknown terrains for uavs. In *2014 IEEE/RSJ International Conference on Intelligent Robots and Systems*, 1742–1747. IEEE.

Sagan, H. (1994). Hilbert's space-filling curve. In *Space-filling curves*, 9–30. Springer.

Seidel, R. (1991). A simple and fast incremental randomized algorithm for computing trapezoidal decompositions and for triangulating polygons. *Computational Geometry*, 1(1), 51–64.

Sklansky, J. and Gonzalez, V. (1980). Fast polygonal approximation of digitized curves. *Pattern recognition*, 12(5), 327–331.

Spires, S.V. and Goldsmith, S.Y. (1998). Exhaustive geographic search with mobile robots along space-filling curves. In *International Workshop on Collective Robotics*, 1–12. Springer.

Tiwari, A., Chandra, H., Yadegar, J., and Wang, J. (2007). Constructing optimal cyclic tours for planar exploration and obstacle avoidance: A graph theory approach. In *Advances in Cooperative Control and Optimization*, 145–165. Springer.

Toussaint, G.T. (1984). A new linear algorithm for triangulating monotone polygons. *Pattern Recognition Letters*, 2(3), 155–158.

Zumbusch, G. (2000). *On the quality of space-filling curve induced partitions*. Citeseer.